

## ESD TEST OF LARGE SOLAR ARRAY COUPON IN GEO PLASMA ENVIRONMENT

**Takashi Kawasaki, Satoshi Hosoda, Jeongho Kim, Mengu Cho**

Department of Electrical Engineering, Kyushu Institute of Technology

1-1 Sensui Tobata-ku Kitakyushu 804-8550, Japan

Phone&Fax: +81-93-884-3229

E-mail: d346411t@tobata.isc.kyutech.ac.jp

### Abstract

The purpose of this research is to investigate the influence of coverglass on arcing phenomena on GEO satellite solar array. Experiments were performed by using a large solar array coupon (400x400mm). The coupon has 50 Si cells. We measured surface potential on the solar array coupon immediately after arc inception. Extent of neutralization differed for each arc. Less charge was neutralized as the distance from arc position increases. At the worst case, 53% charge was neutralized at 325mm in this experiment. Arc plasma propagation velocity was of the order of  $10^4$ m/s but differed widely for each arc.

### Introduction

As scale and duration of space mission becomes large and long, demand for spacecraft electric power has grown up. Recently, solar arrays onboard geostationary orbit (GEO) satellites generate large power (10kW) at high voltage (100V). Because of high voltage power generation, however, short circuit accidents often occur on solar array.[1]

Electric potential of a spacecraft with respect to the surrounding plasma is determined by balance between electrons and ions which flow into the spacecraft. During daytime in GEO, the satellite potential is usually almost zero, governed by photoelectrons of a few eV energy emitted from the spacecraft surface. When a satellite encounters substorm environment, however, its potential becomes extremely negative because of high energy electrons flowing into the satellite. By the difference of secondary emission yield, the potential difference between insulator structures, such as coverglass, and the spacecraft ground appears. The state where the coverglass potential is higher than that of the interconnector that is equal to the spacecraft ground, is called inverted potential gradient. Due to the inverted potential gradient, an arc may occur at the triple junctions where the highest electric fields are formed.[2] The cross-sectional view of spacecraft solar array is shown in Fig. 1.

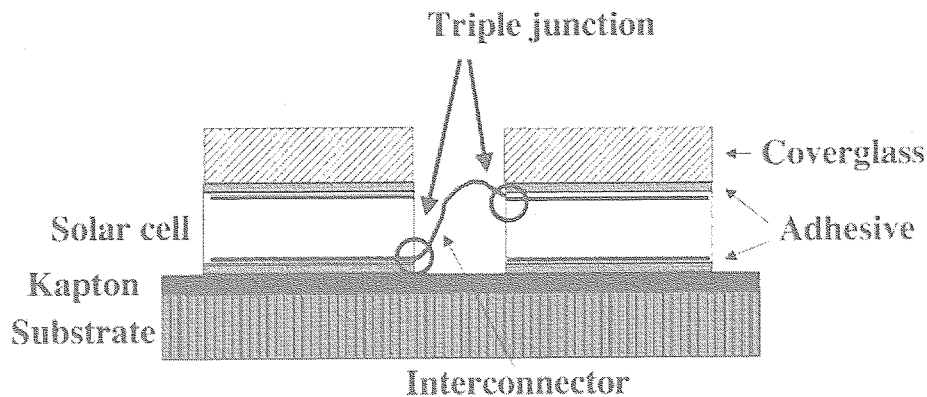


Fig. 1 Schematic picture of cross-section of spacecraft solar array.

If an arc occurs, the energy will be supplied by two types of capacitance, the capacitance of a satellite, and the capacitance of coverglass. The magnitude depends on the size of dielectric materials and satellite. In our laboratory, we have carried out ground tests to evaluate the arc-resistant performance of spacecraft solar array. In the ground test, it is necessary to simulate proper GEO conditions. Making the conditions too severe is not always welcomed, because it leads to increased cost to take superfluous measures based on the test result that might be unnecessary in reality. Since most test facilities are not large enough to accommodate a full solar panel, we usually use coupons in the ground tests. Usually, the capacitance of missing coverglass that is not accommodated in a chamber is simulated by connecting a capacitor to the external circuit. But, there are big differences among research organizations about how much capacitance is appropriate. Demand for the international standard about the ground test conditions is high.

This paper reports results of experiments to investigate the effects of area of coverglass on arcing phenomena in GEO environment. By studying the effect of coverglass area, we can deduce how much of coverglass charge is involved in each arc and how much of coverglass charge should be included in the ground test that uses a small coupon with a limited size. When we suggest the international standard in the ESD ground test of solar array, we need to clarify the following. How much of coverglass charge is involved in each arc? How far does arc plasma propagate? In this paper, we first describe the experimental system. Then, we present the experimental results. Finally we summarize the paper suggesting future work.

### Experiment

#### Solar array coupon

Photographs of the solar array coupon used in the experiments are shown in Fig. 2. The size of coupon is 400x400mm, and the size of each solar cell is 70x35mm. The coupon contains 5 strings and we call the strings as R, B, G, Y and P respectively. They are initials of colors, Red, Blue, Green, Yellow and Purple. The coupon has 50 Si cells. The coverglass is made of BRR/s-0213.

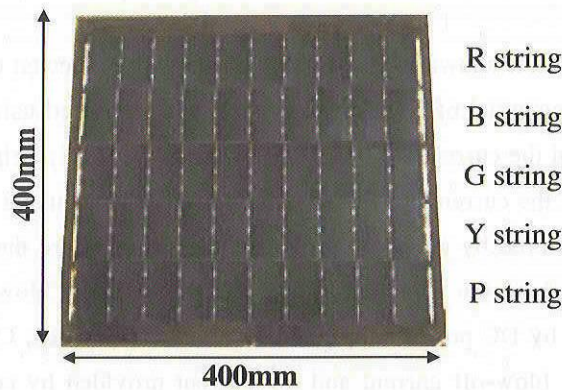


Fig. 2 Photographs of coupon.

### Experimental setup

A schematic picture of the experimental setup is shown in Fig. 3. The experiments were performed in a vacuum chamber with 600mm in diameter and 900mm in length. The pressure in the chamber could be as low as  $1 \times 10^{-4}$  Pa. In order to generate the differential voltage, we biased a coupon to a negative potential using a high voltage power supply (Glassman; EW60kV) and irradiated electron beam on the coupon surface by an electron gun (ULVAC; RHEED). We measured the two-dimensional distribution of the surface potential on the coupon surface using a non-contacting surface potential probe (Trek probe; Model-341) attached to the XY stage controller unit (SIGMAKOKI; SGSP26-150\_200). We identified the position of the arc using a IR camera (SONY; XC-EI50), and an image analysis system.[3] Resistance ( $10\text{M}\Omega$ ) was used to protect the power supply. Since a large coupon was used, we had to make the irradiation area of electron beam expand. Therefore, aluminum foil ( $0.7\mu\text{m}$  thick) was used. The half bandwidth spread by nearly 3 times.[4] The shutter (COPAL; DC-392) was fixed inside the vacuum chamber. The shutter was normal open and operated electronically. If arc occurred, the shutter could be closed immediately, so that we could measure the surface potential on the coupon immediately after an arc while protecting the Trek probe from the electron beam and preserving the charging condition of the surface.

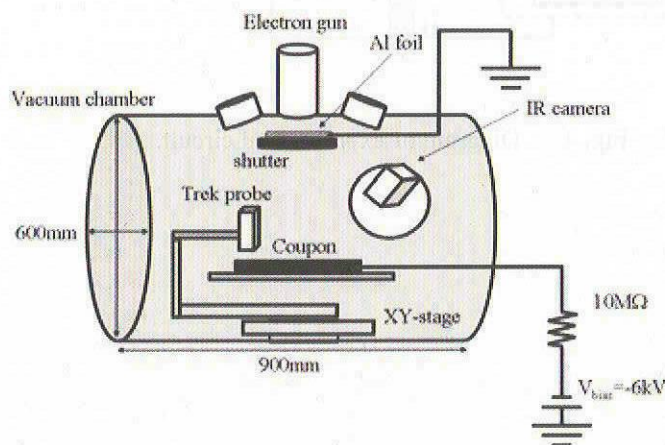


Fig. 3 Schematic picture of Experimental setup.

### Experimental circuit

A diagram of experimental circuit is shown in Fig. 4. The circuit was connected to the solar array coupon via high voltage feed-throughs. The potential of solar array coupon was measured using a high voltage probe, VP (Tektronix; P-5100). We measured the currents to R(CP1), G(CP2) and P(CP3) strings using AC current probes (Tektronix; P6022). We measured the currents to B(CP4) and Y(CP5) strings using DC current probes (HIOKI; 9274). We called the current measured by a current probe for the string where the arc occurred “arc current”. We also call the current measured by the CP6, DC probe (HIOKI; 3274), “blow-off current”. The blow-off current was the current provided by DC power supply and external capacitance,  $C_{ext}$ , only. On the other hand, the arc current is the sum of the blow-off current and the current provided by coverglass capacitance of the other strings, which we called “neutralization current”. When the arc occurred, electron was emitted from the arc spot. Then, coupon potential rose rapidly toward zero. We used this as a trigger source. The high voltage probe was connected to a trigger generator oscilloscope (LeCroy; wave surfer 424). This oscilloscope sent trigger signals to the oscilloscope-1 (Tektronix; TDS2014), the oscilloscope-2 (Tektronix; TDS224) and the shutter. Waveform data of oscilloscopes were saved to PC via GPIB cable. A typical waveform is shown in Fig. 5.

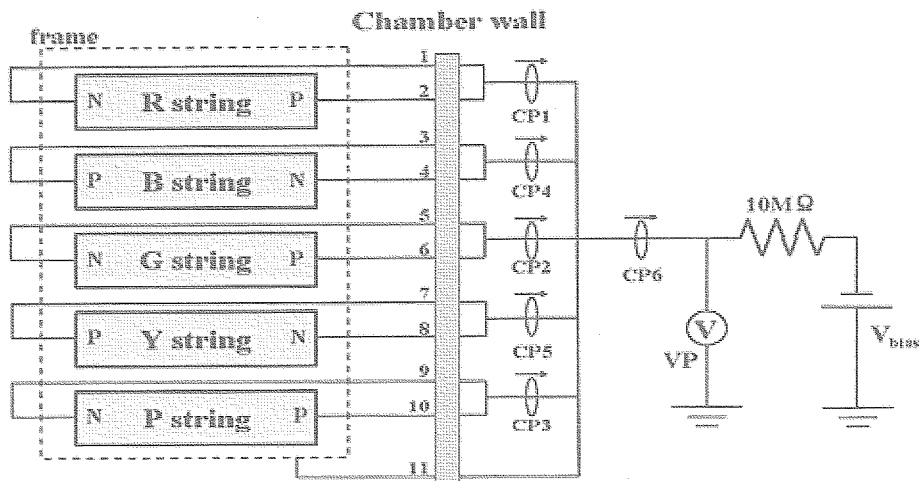


Fig. 4 Diagram of experimental circuit.

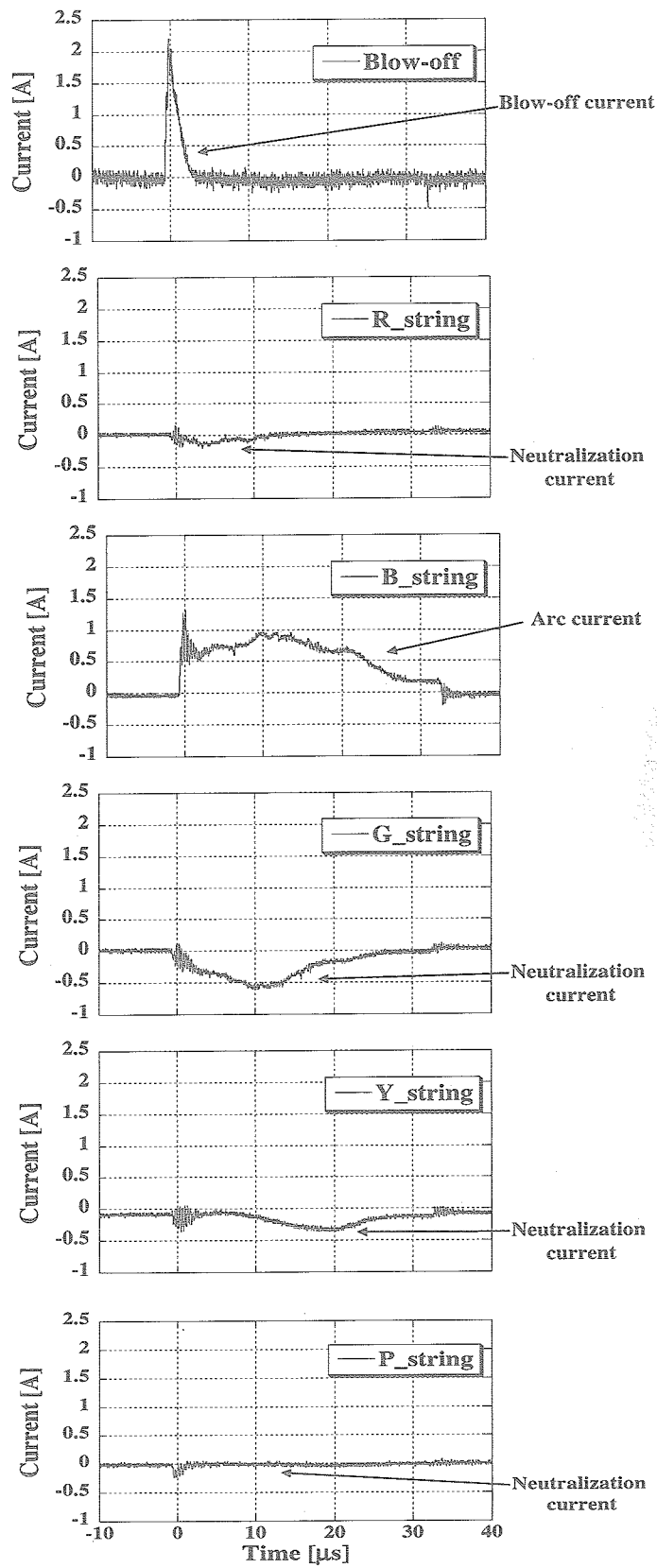


Fig. 5 Typical waveform measured in the current probe shown in Fig. 4.

## Results and discussions

### Measurement of surface potential at specific points

We describe the study on the propagation distance. We measured the surface potential at specific point at a regular interval. Electron beam irradiated the coupon for 30 seconds the shutter blocked it during the measurement of the surface potential. If an arc occurred during 30 seconds, shutter was closed immediately and measured the surface potential. Surface potential measurements were performed at point1 and point2 shown in Fig. 6. Change of surface potential is shown in Fig. 7.

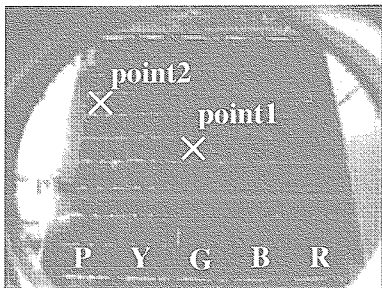


Fig. 6. Measurement point.

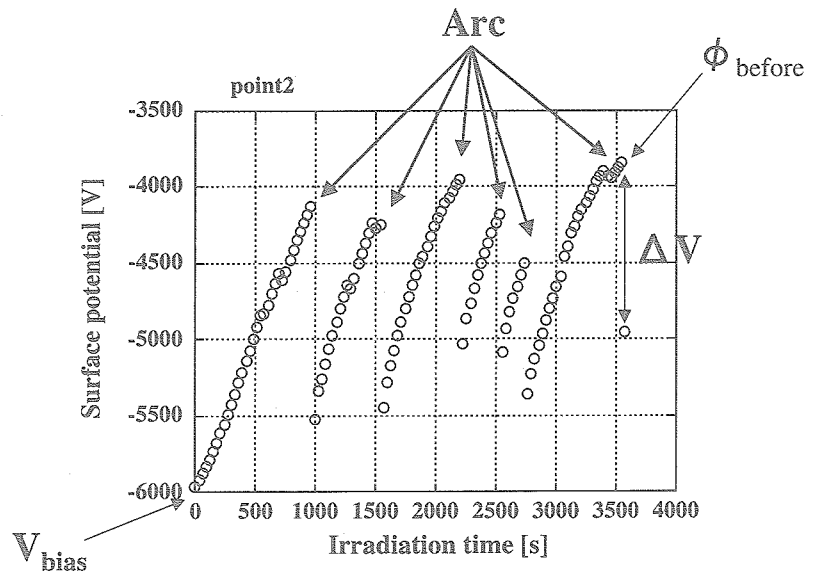


Fig. 7. Change of surface potential at point2.

First, surface potential on coverglass is the same as the bias voltage that is  $-6\text{kV}$ . The surface potential rises by electron beam irradiation. When the differential voltage becomes larger, an arc occurs. The coverglass surface is neutralized by arc plasma. Then, the surface potential drops rapidly. Here,  $\phi_{\text{before}}$  is the potential immediately before arc, and  $\Delta V$  is the potential change after arc.

Relation between  $\Delta V$  and the neutralization current charge at the measured string is shown in Fig. 8. When the measurement point is point1, neutralization current charge is the time integration of the G string current. On the other hand, when the measurement point is point2, neutralization current charge is the time integration of the P string current. As the graph indicates, there is a strong correlation between them. The result clearly shows that neutralization current is provided by coverglass capacitance. Difference of gradient between point1 and point2 is probably due to charging condition.

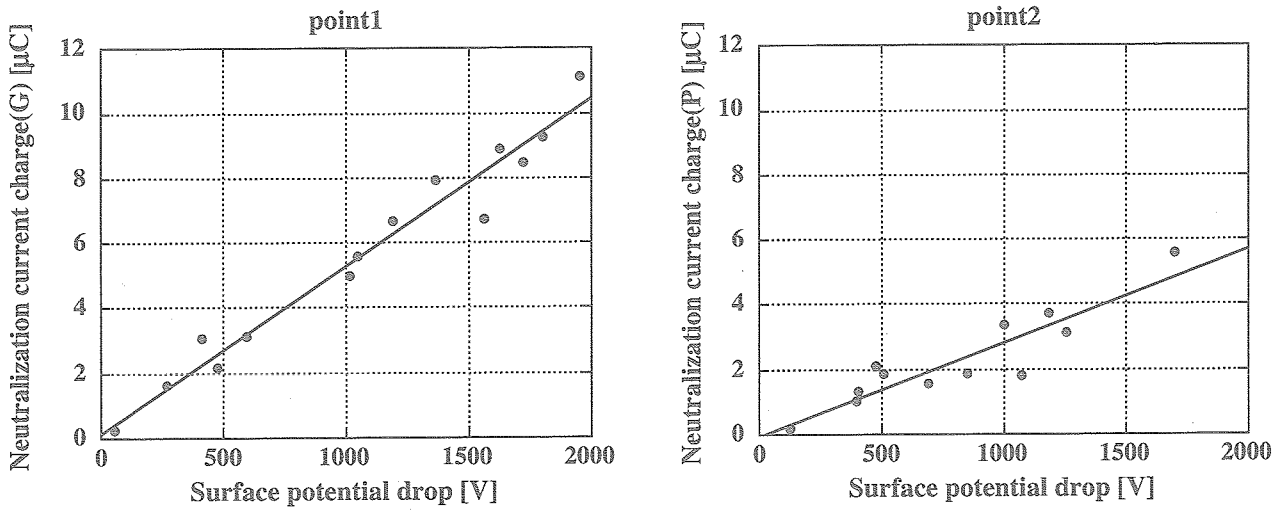


Fig. 8. Relation between  $\Delta V$  and the neutralization current charge at the measured string.

Next, relation between the distance from arc position and the neutralized ratio is shown in Fig. 9. The horizontal axis shows the distance from the arc position to the measurement points. The vertical axis corresponds to the ratio of the potential change ( $\Delta V$ ) to the differential voltage ( $\phi_{\text{before}} - V_{\text{bias}}$ ) before arc inception. If surface potential drops to  $-6\text{kV}$  by arc, it is 100%. In the case where the arc position is near the measurement point, almost all the charge is neutralized. Less charge is neutralized as the distance from arc position increases. The cases where charge is not neutralized exist in 300-350mm. There are several arcs that neutralization ratios are different in the vicinity of 300mm. This means that extent of neutralization differs for each arc. At the worst case, 53% charge was neutralized at 325mm.

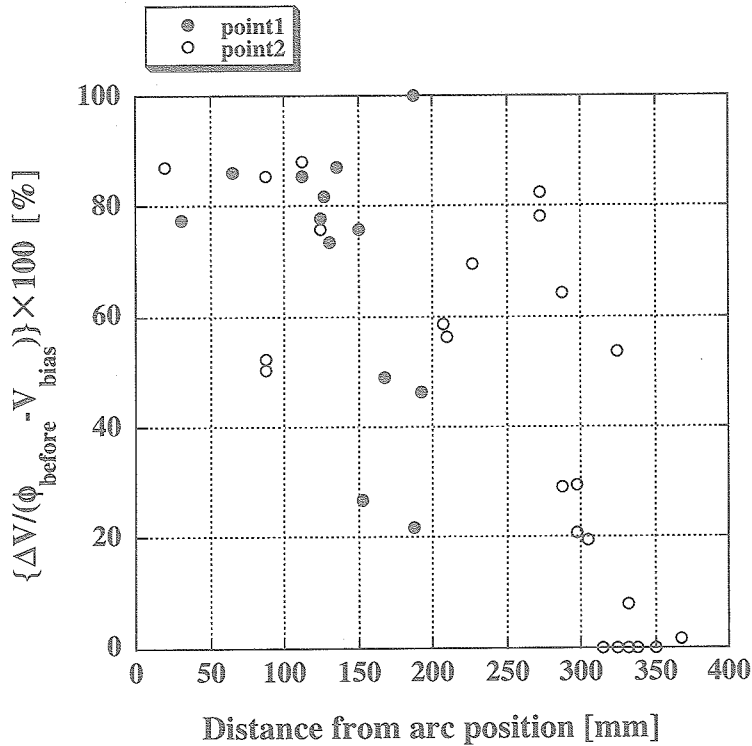


Fig. 9. Relation between the distance from arc position and the neutralized ratio.

### Arc plasma propagation velocity

If arc plasma propagation velocity is determined, the pulse width of arc current at real satellite can be estimated. According to Ref. [5], the arc plasma propagation velocity is  $9.0 \times 10^3$  [m/s]. We calculate the velocity from the delay time of neutralization current. The waveform of an arc which occurred at the B string is shown in fig. 10. There is a time delay of  $10 \mu\text{s}$  between the neutralization current peaks of G string and Y string. Since the length of a cell is 70mm, we can calculate the arc plasma propagation velocity as follows.

$$V_p = \frac{0.07[m]}{t} = \frac{0.07[m]}{10[\mu s]} = 0.7 \times 10^4 [m / s]$$

The velocity of this case is the slowest. The fastest is  $14 \times 10^4$  [m/s]. The arc plasma propagation velocity is of the order of  $10^4$  m/s but differs for each arc.

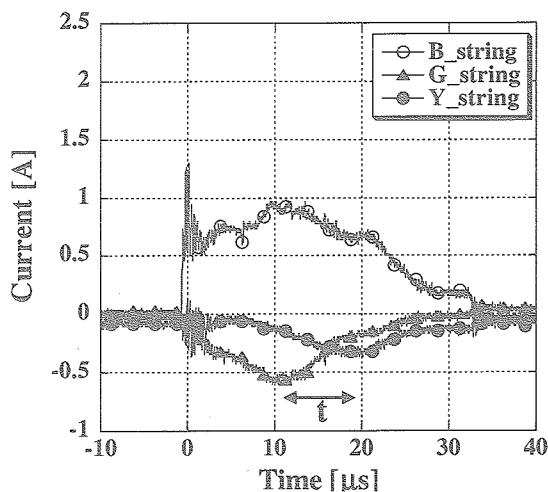


Fig. 10. Arc current waveform.

### Summary

We performed solar array ESD experiments with a large-scale solar array coupon to establish the international standard in the ESD ground test of solar array.

1. Neutralization current is provided by charge on coverglass. Extent of neutralization differs for each arc.
2. Less charge is neutralized as the distance from arc position increases. At the worst case, 53% charge was neutralized at 325mm in this experiment.
3. Arc plasma propagation velocity is of the order of  $10^4$  m/s but differs for each arc.

We need more experimental data of the surface potential immediately after arc inception. We need to examine whether there is an arc that neutralizes all the charges stored in 50 cells.



### Acknowledgement

Authors thank Sharp Corporation and Alcatel Space for providing the large coupon. Discussion with Denis Payan and Emanuel Amorim of CNES, Leon Levy, Rene Reulet of ONERA is also appreciated.

### References

- [1] Katz, I., Davis, V.A; and Snyder, D.B. "Mechanism for Spacecraft Charging Initiated Destruction of Solar Arrays in GEO", AIAA 98-1002, 36<sup>th</sup> Aerospace Sciences Meeting & Exhibit, Reno, January, (1998)
- [2] Cho, M., and Fujii, H., "Review on Charging and Discharge Phenomena in Space Environment: Arcing on High Voltage Solar Array and Future Issues", Aeronautical and Space Sciences Japan, Vol.51, pp.139-145, (2003)
- [3] Toyoda, K., Cho, M., and Hikita, M., "Development of Position Identification System of Arc Discharge on a Solar Array in Vacuum by Digital Processing of Video Images", Journal of the Japan Society for Aeronautical and Space Sciences, Vol.51, No.589, pp.82-84, (2003)
- [4] Kawasaki, T., Shikata, Y., Hosoda, S., Kim, J., and Cho, M., "Influence of Coverglass on Arcing Phenomena on GEO Satellite Solar Array", 24<sup>th</sup> International Symposium on Space Technology and Science, Miyazaki, June, (2004)
- [5] Leung, P., "Plasma Phenomena Associated with Solar Array Discharges and Their Role in Scaling Coupon Test Results to a Full Panel", AIAA 2002-0628, 40<sup>th</sup> Aerospace Sciences Meeting & Exhibit, Reno, January, (2002)